Journal of the European Ceramic Society 45 (2025) 117566

Contents lists available at ScienceDirect

Journal of the European Ceramic Society

journal homepage: www.elsevier.com/locate/jeurceramsoc

Elastic properties of domains and domain walls in $(K_{0.5}Na_{0.5})NbO_3$ single crystal

Katarina Žiberna [a,b,*], Maja Koblar [a], Andraž Bradeško [a], Micka Bah [c], Franck Levassort [c], Goran Dražić [d], Hana Uršič [a,b], Andreja Benčan [a,b,*]

[a] Electronic Ceramics Department, Jožef Stefan Institute, Ljubljana 1000, Slovenia
[b] Jožef Stefan International Postgraduate School, Ljubljana 1000, Slovenia
[c] GREMAN UMR7347, Université de Tours, CNRS, INSA CVL, Tours 37071, France
[d] Department of Materials Chemistry, National Institute of Chemistry, Ljubljana 1000, Slovenia

ARTICLE INFO

Keywords:
Elasticity
Ferroelectrics
Potassium sodium niobite
Domains
Domain walls

ABSTRACT

The elastic properties of ferroelectric materials at the nanoscale are intricate, with domains and domain walls each having their own distinct elasticity – a property which can be exploited for tailoring materials performance. In this study, we report on the elastic response of the ferroelectric domain structure of a $(K_{0.5}Na_{0.5})NbO_3$ single crystal, measured using an atomic force microscopy-based techniques. Before mapping the elastic properties, the domain structure was characterized using piezo-response force microscopy and transmission electron microscopy. The average measured reduced elastic modulus was ~130 GPa. The 90° domain walls exhibit a 20 % difference in the reduced modulus, appearing elastically harder on one side of the domain and elastically softer on the other. In contrast, 60° domain walls showed no mechanical contrast with the neighboring domains. Anisotropy in elasticity was also observed between domains with different piezoelectric activity.

1. Introduction

Distinct properties of domain walls (DWs) in ferroelectric materials are one of the key aspects driving their research for use in nanotechnological applications [1]. The structural differences between these quasi-2-D defects and the domains they separate give rise to a variety of properties that differ in bulk, such as altered electrical properties like increased conductivity [2,3].

A far less investigated property are DWs' mechanical characteristics. The nanometric width of DWs, poses a challenge in mechanical testing, and limits the number of techniques to a selected few, possessing high enough spatial resolution and the ability to measure mechanical properties. Most commonly used are atomic force microscopy (AFM)-based techniques, i.e., ultrasonic AFM, acoustic AFM, force-distance curves, offering non-destructive measurements of elastic properties at the nanoscale level, as well as the study of stress induced nanoscale phenomena [4].

DWs separate domains of different direction of the ferroelectric polar order called spontaneous polarization ($\vec{P_s}$). Depending on the symmetry of the ferroelectric phase, several different types of DWs can be found in the material, which can be classified by the angle formed between the $\vec{P_s}$ vectors in two neighboring domains, and can have different elastic properties. 180° DWs were reported to be elastically softer, i.e. have a lower elastic modulus, than the adjacent domains in periodically poled lithium niobate, $BaTiO_3$ and $PbTiO_3$ [5–7]. The elastic softening of 10–20 % was found to be independent of the morphology and composition of the samples. Interestingly, elastic softening was only observed for 180° DWs separating domains with out-of-plane $\vec{P_s}$, i.e. domains with $\vec{P_s}$ perpendicular to the sample's surface, while 180° DWs separating domains with in-plane $\vec{P_s}$, domains where $\vec{P_s}$ lies parallel to the sample surface, showed no elastic contrast. In addition, anisotropy between different domains was reported in $BaTiO_3$ and $PbTiO_3$. The in-plane domains exhibited higher elastic modulus compared to the out-of-plane domains, which highlights the importance of the absolute direction of $\vec{P_s}$ [7,8].

90° DWs in $PbTiO_3$ which are, in addition to being ferroelectric, also ferroelastic, with valley and ridge topography were observed to have a higher or a lower modulus than the adjacent domains. The variations of the modulus occured only when the $\vec{P_s}$ of one of the neighboring

* Corresponding authors at: Electronic Ceramics Department, Jožef Stefan Institute, Ljubljana 1000, Slovenia.
E-mail addresses: katarina.ziberna@ijs.si (K. Žiberna), andreja.bencan@ijs.si (A. Benčan).

https://doi.org/10.1016/j.jeurceramsoc.2025.117566
Received 18 December 2024; Received in revised form 25 April 2025; Accepted 26 May 2025
Available online 27 May 2025

domains was pointing out-of-plane (*a*-*c* DWs) [8,9].

The cause for the distinct mechanical DW behavior is still not clear. Some proposed contributions include defects segregated at the DWs [6,9], topography changes associated with twinning [8,9], DW tilt [8], strain states at different DWs [8], depolarization fields created by AFM tip pressure at the DW [7] and local DW movements at the surface under the AFM tip of both ferroelectric and ferroelastic DWs that result in elastic softening of the material [7]. The latter contribution can be especially concerning, as it can mask the intrinsic elastic hardening due to DW motion [9].

The different elastic properties of DWs have already attracted interest and suggestions have been made as to where this phenomenon could be exploited, for example they could be utilized to modulate thermal conductivity through the bulk [7,9–11]. At the surface, these properties could enable the mechanical detection of DWs in highly conductive materials where traditional probing methods are ineffective [7]. Additionally, in life sciences, the ability to control surface elasticity could influence bacterial adhesion, which is known to depend on the elastic properties of the surface [9]. Furthermore, domain engineering can be used to produce a material with a favorable modulus of elasticity by exploiting the elastic anisotropy of the differently oriented domains.

$(K_{0.5}Na_{0.5})NbO_3$ (KNN) and KNN-based compositions are investigated as potential lead-free alternatives to Pb(Zr, Ti)O_3-based ferroelectrics, not only due to the comparable piezoelectric activity and higher Curie temperature of 420 °C [12], but also because of the higher elastic modulus, which makes KNN and its derivatives more suitable for ultrasonic applications [13].

Here we look at the local elastic properties of domains and DWs in a KNN single crystal prepared by solid-state crystal growth [14,15] using Peak Force Quantitative NanoMechanical mapping (PF-QNM). Prior to mapping the elastic properties, the domain structure was characterized using a combination of off-resonance vector piezo-response force microscopy (PFM), cross-sectional transmission electron microscopy (TEM) and crystallographic orientation mapping.

2. Methods

The KNN sample prepared by solid-state crystal growth [14,15] was cut, polished with SiC grading papers and 3-μm and 0.25-μm diamond paste. To achieve a mirror-like surface finish and remove near-surface defects caused by mechanical polishing, the sample was additionally polished with colloidal silica for 2 hours. The polished surface was determined to be close to the (100) plane according to electron backscattered diffraction (EBSD) (Supplementary Materials, S1). EBSD and transmission Kikuchi diffraction (TKD) were performed in a scanning electron microscope Apreo 2 S (Thermo Fischer Scientific, Waltham, MA, USA) equipped with an EBSD analyzer C-Swift (Oxford Instruments, Abingdon, UK) at 30 kV. For EBSD, the sample was tilted at 70°, while for TKD the transparent sample was tilted for −20°. The diffraction patterns were indexed with the space group *Bmm*2 [16] in the AZtecCrystal program (Oxford Instruments, Abingdon, UK). The difference in orientation between two neighboring domains were determined by rotation of the coordinate system of one domain to the coordinate system of the neighboring domain using the transposed rotation matrix [17,18].

The off-resonance vector PFM mappings were done with a Bruker Dimension Icon (Bruker Nano Surfaces, Santa Barbara, CA, USA) using a DDESP-V2 probe coated with doped diamond (Bruker Nano Surfaces, Santa Barbara, CA, USA) with a nominal radius of 100 nm and a cantilever spring constant of 80 N/m. The driving voltage and frequency were 2 V and 15 kHz, respectively, while the scan rate was set to 0.3 Hz.

The PF-QNM was performed in a Bruker Dimension Icon (Bruker Nano Surfaces, Santa Barbara, CA, USA) with a diamond AFM probe DNISP-HS with a cube-corner geometry having a nominal tip radius of 40 nm and a cantilever spring constant of 353 N/m (Bruker Billerica, MA, USA). To gain a quantitative reduced elastic modulus, the deflection sensitivity and the effective tip radius were calibrated on sapphire and fused silica, respectively. The force applied during the measurement was 3 μN. PF-QNM is a tapping technique that makes a force-distance curve at each pixel of the image, allowing the extraction of the elasticity modulus [19].

After PFM and PF-QNM, a transparent lamella was prepared from the region of interest using a gallium source focused ion beam Helios Nanolab 650 HP (Thermo Fischer Scientific, Waltham, MA, USA). The bright field TEM images and the selected area electron diffractions (SAED) were acquired on a JEM 2100 (Jeol, Tokyo, Japan) operated at 200 kV.

3. Results and discussion

The 12 possible directions of $\overrightarrow{P_s}$ in KNN along $[110]_{pc}$ can give rise to four types of DWs, 180°, 120°, 90° and 60° DWs [20]. The domain structure can thus be fairly complex, composed of herringbone [21–24], watermarks [21–23] and zig-zag [23–25] patterns.

Fig. 1 presents the domain structure in the region of interest, probed using vector PFM, with a measured surface roughness of 1.6 nm (Fig. 1a). The domain structure consists of larger lamellar domains of approximately 2–2.5 μm in width (Fig. 1b-e, yellow arrows) with a substructure of smaller lamellar domains of less than 1 μm in width (Fig. 1b-e, white arrows) that extend over the larger domains.

Fig. 1b-e shows two components of the $\overrightarrow{P_s}$, the out-of-plane component (P_z) and one in-plane component (P_y), revealing a complex piezoelectric activity. The in-plane signal (Fig. 1b, c) of the larger domains appears to change the polar direction over the DW (marked with yellow arrows), while the out-of-plane component of $\overrightarrow{P_s}$ (Fig. 1d, e) does not change neither amplitude nor direction, which is indicative of non-180° DWs.

The smaller domains (marked with white arrows), however, have no PFM in-plane phase signal and zero in-plane amplitude signal (Fig. 1b, c). Once the smaller domains cross DWs separating the larger domains (marked with yellow arrows), the out-of-plane amplitude and phase change (Fig. 1d, e), indicating that the out-of-plane component of $\overrightarrow{P_s}$ changes directions, but not for 180° as the out-of-plane amplitude is different in the neighboring domains.

In cross-section, i.e., in the direction roughly perpendicular to the sample's surface, the regions of interest's domain structure appeared to have a zig-zag pattern (Fig. 2a). We have identified the domains that are inclined by about 10° with respect to the surface (Fig. 2a) as the larger domains highlighted with yellow arrows in Fig. 1. The smaller domains, marked with white arrows in Fig. 1, were observed to intersect the larger domains in a zig-zag-like fashion.

According to TEM and TKD (Fig. 2a, b, respectively), the DWs separating larger domains parallel to $(100)_{pc}$ planes are 90° DWs (Fig. 2a, yellow arrows), while DWs separating smaller domains (Fig. 2a, white arrows), are either 60° or 120° DWs, which cannot be separated during orientation indexing [17]. In addition, the DWs confining the smaller domains are not parallel to one of the expected $(110)_{pc}$ planes, suggesting their type is either uncharged 60° DW or charged 120° DWs, as they can occupy a random plane defined by the piezoelectric and electrostatic coefficients of the material [26].

The results are in line with the PFM analysis (Fig. 1). Assuming the favorable formation of neutral DWs, we conclude that the larger domains are thus separated by 90° DWs, while the smaller domains are separated by 60° DWs. This conclusion is further supported by comparing experimental SAED patterns over these DWs with the simulated ones, with the domain structure sketch provided in the Supplementary Materials (Supplementary Materials, S2).

Fig. 3 shows the map of the reduced elastic modulus for the same region of interest as in Fig. 1, obtained using PF-QNM, a technique based on the same principles as those previously used to probe the elastic properties of both domains and DWs [8]. The average value of the

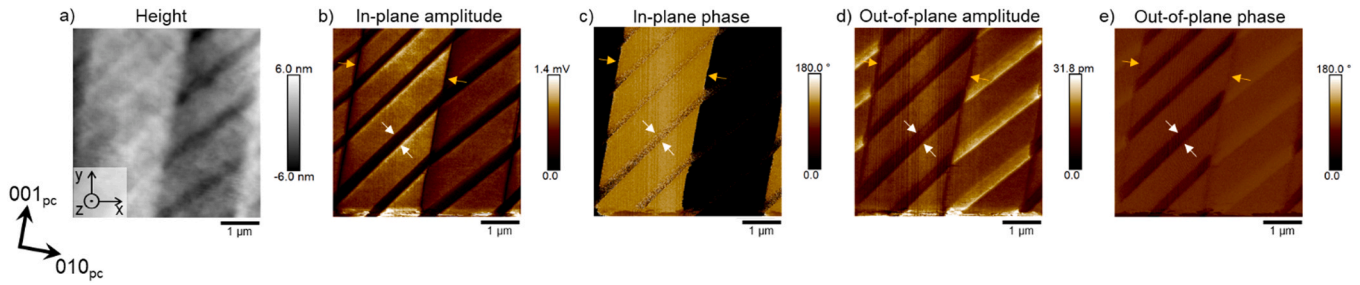

Fig. 1. PFM of the region of interest in the KNN single crystal: a) topography, b) in-plane PFM amplitude, c) in-plane PFM phase, d) out-of-plane PFM amplitude, e) out-of-plane PFM phase. Yellow and white arrows point to domain with similar morphology.

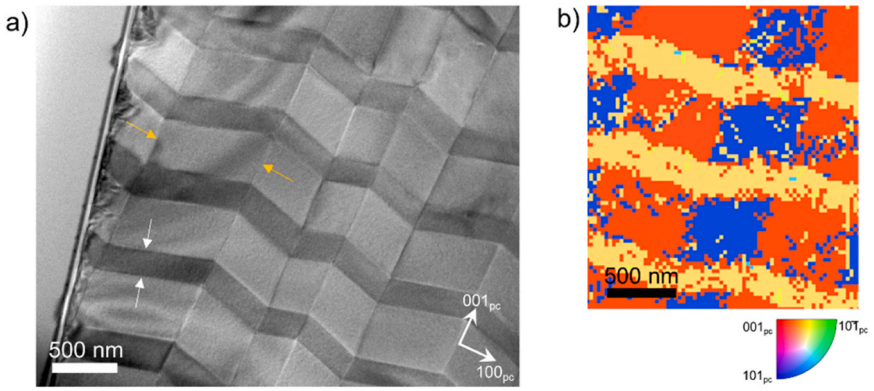

Fig. 2. a) TEM image of the KNN domain structure in cross-section. The yellow and white arrows mark the same types of domain as in Fig. 1; b) Filtered TKD orientation map of a part of the image in a and the corresponding inverse-pole figure legend. The TKD patterns were indexed with the space group *Bmm*2 [16] in the orthorhombic metric, which was then converted into pseudocubic notations.

reduced modulus obtained from the image is ~130 GPa, which agrees well with the reduced elastic modulus determined using nano-indentation (Supplementary Materials, S3). The three line profiles of the reduced modulus, along with the height profile, were extracted to see the correlation between the reduced modulus and changes in polarity direction in KNN (Fig. 1). One line profile was taken over a larger domain separated by 90° DWs (Fig. 3, labeled I) and two taken perpendicular over smaller domains separated by 60° DWs (Fig. 3, labeled II and III).

The line profile taken perpendicular to the 90° DWs separating larger domains (Fig. 3, label I) shows a significant variation in the reduced modulus on DWs separating larger domains. The variation of the modulus measured in between the DW of ± 4 % is regarded as noise. Interestingly, on one side of the domain, the DW exhibits a reduced modulus which is lower than that measured within domains, while on the opposite side, the DW shows a higher reduced modulus (Fig. 3, yellow arrows). The difference in the elastic modulus between the domains and DWs is approximately ± 20 %, which aligns well with other experimental measurements where differences up to ~28 % were observed between domains and DWs [8]. Additionally, the elastic softening and hardening effects were observed to extend over ~100 nm into the domain, likely due to the interactions between DWs and the surface, which may alter the stress/strain states and result in widening of the DW at the surface [27]. The widening can also be explained by the inclination of the DW relative to the surface, i.e., the DW not being measured edge on.

Based on the literature, the measured elastic contrast at the DWs can result from a combination of intrinsic elastic properties of DWs and extrinsic contributions. First, we rule out topographical effects, as in our case, surface variations are minimal, with gradual, non-abrupt changes ranging from 0.5 nm to 1.5 nm (Fig. 3 and Supplementary Materials, S4). Second, we exclude DW motion as a contributing factor, since such motion would uniformly soften the elastic response of all DWs, regardless of their intrinsic properties [7,9].

The intrinsic elastic response of 90° DWs is likely linked to variations in strain states at the as suggested by He et al., who, using molecular dynamics simulation, observed a slight variation (± 0.7 %) in the elastic modulus at ferroelastic 90° DWs with ridge and valley topography. [9]. As our material is ferroelectric, the 90° DWs investigated are in addition to being ferroelastic, also ferroelectric in character. The continuous change of $\vec{P_s}$ across the DWs may contribute to the measured elasticity through electromechanical effects triggered by the inhomogeneous stress fields under the AFM probe. Additionally, the favorable orientation of the surrounding domains plays a crucial role in detecting the DWs elastically. Specifically, when the adjacent domains have an out-of-plane $\vec{P_s}$ component, the DWs can be observed in elasticity measurements. In contrast, if the DWs were confined between purely in-plane $\vec{P_s}$ domains, their elastic contrast would not be detectable [7,8].

For the smaller domains (Fig. 3, labels II and III), a decrease in the reduced modulus of approximately 10–20 % was observed compared to the neighboring domains. The difference is likely due to a different direction of $\vec{P_s}$ within domains, similarly to what has been observed in ferroelectrics with a structure of higher symmetry, namely tetragonal $BaTiO_3$ and $PbTiO_3$. In these materials, the direction of $\vec{P_s}$ was directly correlated with the elastic modulus, where domains with out-of-plane $\vec{P_s}$ exhibit a lower elastic modulus than those with in-plane $\vec{P_s}$ [7,8,28]. However, due to the lower symmetry of the orthorhombic structure compared to the tetragonal structure, the elastic anisotropy of KNN is more complex, as shown in Figure S5 [29]. This complexity is especially pronounced when measurements are taken along non-low-zone axes, making it challenging to interpret the $\vec{P_s}$ direction solely based on the reduced elastic modulus.

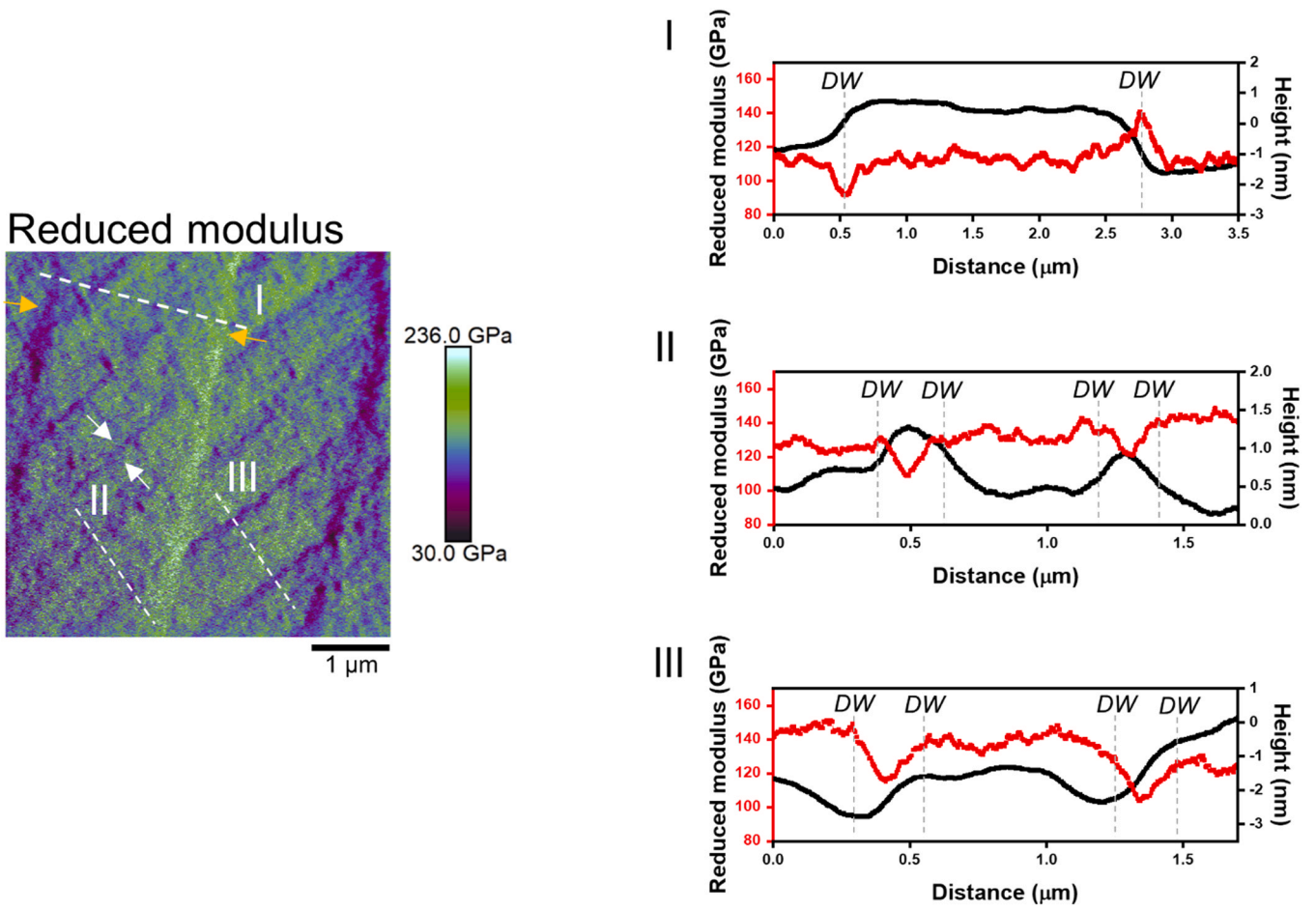

Fig. 3. Map of the reduced elastic modulus with line profiles taken over a larger domain (I) and smaller domains (II, III) accompanied by the height profiles. The positions of the DWs in the line profiles were determined from the PFM images in Fig. 1 and are marked by grey dashed lines.

The 60° DWs confining these smaller domains show no distinct elastic contrast. Although for 90° DWs mainly stress and strain are discussed as the main causes of their pronounced elastic response [8,9], in reality many properties such as structure and morphology, in addition to strain, contribute to their elastic response through electromechanical and mechanical contributions and are needed to determine the origin of the particular elasticity at the DWs.

4. Conclusions

In summary, this work shows the complex elastic response of KNN at the nanoscale. For the first time, the elastic properties in KNN were measured over 90° and 60° DWs, where 90° DWs show an increase in elasticity from the average reduced modulus of 130 GPa on one side of the domain and a decrease on the other side, while 60° DW shows no elastic contrast. Furthermore, anisotropy of the reduced elastic modulus was observed across domains with different piezoelectric activity. The orthorhombic symmetry does not allow for a straightforward interpretation of the $\vec{P_s}$ direction based on the elastic modulus, as is possible with tetragonal ferroelectrics.

CRediT authorship contribution statement

Andraž Bradeško: Writing – review & editing, Investigation, Formal analysis, Data curation. **Franck Levassort:** Writing – review & editing, Investigation, Funding acquisition. **Micka Bah:** Writing – review & editing, Investigation, Formal analysis, Data curation. **Maja Koblar:** Writing – review & editing, Investigation, Formal analysis. **Katarina Žiberna:** Writing – original draft, Visualization, Validation, Investigation, Formal analysis, Data curation, Conceptualization. **Hana Uršič:** Writing – review & editing, Validation, Investigation, Funding acquisition, Conceptualization. **Goran Dražić:** Writing – review & editing, Investigation. **Andreja Benčan:** Writing – review & editing, Validation, Supervision, Resources, Project administration, Investigation, Funding acquisition, Conceptualization.

Declaration of Competing Interest

The authors declare that they have no known competing financial interests or personal relationships that could have appeared to influence the work reported in this paper.

Acknowledgement

This work is supported by the Slovenian Research and Innovation Agency through core funding (project P2–0105), national postgraduate funding (project PR-10481), project J7–4637 and bilateral project BI-FR/22–23-PROTEUS-10. Val Fišinger is acknowledged for the help with the atomic force microscope.

Appendix A. Supporting information

Supplementary data associated with this article can be found in the online version at doi:10.1016/j.jeurceramsoc.2025.117566.

References

[1] D. Meier, S.M. Selbach, Ferroelectric domain walls for nanotechnology, Nat. Rev. Mater. 7 (2022) 157–173, https://doi.org/10.1038/s41578-021-00375-z.

[2] J. Seidel, L.W. Martin, Q. He, Q. Zhan, Y.H. Chu, A. Rother, M.E. Hawkridge, P. Maksymovych, P. Yu, M. Gajek, N. Balke, S.V. Kalinin, S. Gemming, F. Wang, G. Catalan, J.F. Scott, N.A. Spaldin, J. Orenstein, R. Ramesh, Conduction at domain walls in oxide multiferroics, Nat. Mater. 8 (2009) 229–234, https://doi.org/10.1038/nmat2373.

[3] T. Rojac, A. Bencan, G. Drazic, N. Sakamoto, H. Ursic, B. Jancar, G. Tavcar, M. Makarovic, J. Walker, B. Malic, D. Damjanovic, Domain-wall conduction in ferroelectric $BiFeO_3$ controlled by accumulation of charged defects, Nat. Mater. 16 (2017) 322–327, https://doi.org/10.1038/nmat4799.

[4] Y. Heo, P. Sharma, Y.Y. Liu, J.Y. Li, J. Seidel, Mechanical probing of ferroelectrics at the nanoscale, J. Mater. Chem. C. 7 (2019) 12441–12462, https://doi.org/10.1039/c9tc02661d.

[5] T. Tsuji, H. Ogiso, J. Akedo, S. Saito, K. Fukuda, K. Yamanaka, Evaluation of domain boundary of piezo/ferroelectric material by ultrasonic atomic force microscopy, Jpn. J. Appl. Phys., Part 1 Regul. Pap. Short. Notes Rev. Pap. 43 (2004) 2907–2913, https://doi.org/10.1143/JJAP.43.2907.

[6] T. Tsuji, S. Saito, K. Fukuda, K. Yamanaka, H. Ogiso, J. Akedo, Y. Kawakami, Significant stiffness reduction at ferroelectric domain boundary evaluated by ultrasonic atomic force microscopy, Appl. Phys. Lett. 87 (2005) 071909, https://doi.org/10.1063/1.2012537.

[7] C. Stefani, L. Ponet, K. Shapovalov, P. Chen, E. Langenberg, D.G. Schlom, S. Artyukhin, M. Stengel, N. Domingo, G. Catalan, Mechanical softness of ferroelectric 180° domain walls, Phys. Rev. X. 10 (2020) 41001, https://doi.org/10.1103/PhysRevX.10.041001.

[8] C.P.T. Nguyen, P. Schoenherr, J. Seidel, Intrinsic mechanical compliance of 90° domain walls in $PbTiO_3$, Adv. Funct. Mater. 33 (2023) 2211906, https://doi.org/10.1002/adfm.202211906.

[9] X. He, X. Ding, J. Sun, G.F. Nataf, E.K.H. Salje, Elastic softening and hardening at intersections between twin walls and surfaces in ferroelastic materials, APL Mater. 11 (2023) 071114, https://doi.org/10.1063/5.0159836.

[10] J.F. Ihlefeld, B.M. Foley, D.A. Scrymgeour, J.R. Michael, B.B. McKenzie, D. L. Medlin, M. Wallace, S. Trolier-Mckinstry, P.E. Hopkins, Room-temperature voltage tunable phonon thermal conductivity via reconfigurable interfaces in ferroelectric thin films, Nano Lett. 15 (2015) 1791–1795, https://doi.org/10.1021/nl504505t.

[11] P.E. Hopkins, C. Adamo, L. Ye, B.D. Huey, S.R. Lee, D.G. Schlom, J.F. Ihlefeld, Effects of coherent ferroelastic domain walls on the thermal conductivity and Kapitza conductance in bismuth ferrite, Appl. Phys. Lett. 102 (2013) 121903, https://doi.org/10.1063/1.4798497.

[12] Y. Saito, H. Takao, T. Tani, T. Nonoyama, K. Takatori, T. Homma, T. Nagaya, M. Nakamura, Lead-free piezoceramics, Nature 432 (2004) 84–87, https://doi.org/10.1038/nature03028.

[13] K. Uchino, Glory of piezoelectric perovskites, Sci. Technol. Adv. Mater. 16 (2015) 46001, https://doi.org/10.1088/1468-6996/16/4/046001.

[14] J.G. Fisher, A. Benčan, M. Kosec, S. Vernay, D. Rytz, Growth of dense single crystals of potassium sodium niobate by a combination of solid-state crystal growth and hot pressing, J. Am. Ceram. Soc. 91 (2008) 1503–1507, https://doi.org/10.1111/j.1551-2916.2008.02324.x.

[15] A. Benčan, E. Tchernychova, M. Godec, J. Fisher, M. Kosec, Compositional and structural study of a $(K_{0.5}Na_{0.5})NbO_3$ single crystal prepared by solid state crystal growth, Microsc. Micro 15 (2009) 435–440, https://doi.org/10.1017/S1431927609090722.

[16] N. Ishizawa, J. Wang, T. Sakakura, Y. Inagaki, K.I. Kakimoto, Structural evolution of $Na_{0.5}K_{0.5}NbO_3$ at high temperatures, J. Solid State Chem. 183 (2010) 2731–2738, https://doi.org/10.1016/j.jssc.2010.09.018.

[17] H.-J. Bunge, Texture Analysis in Materials Science, Butterworth & Co, Berlin, Germany, 1982, https://doi.org/10.1016/C2013-0-11769-2.

[18] K. Žiberna, M. Koblar, M. Bah, F. Levassort, G. Dražić, H. Uršič, A. Benčan, Nanomechanical characterization of $BiFeO_3$ ferroelectric ceramics, J. Eur. Ceram. Soc. 44 (2024) 7025–7031, https://doi.org/10.1016/j.jeurceramsoc.2024.05.011.

[19] A. Kwaśniewska, M. Świetlicki, A. Prószyński, G. Gładyszewski, The quantitative nanomechanical mapping of starch/kaolin film surfaces by peak force afm, Polymers 13 (2021) 244, https://doi.org/10.3390/polym13020244.

[20] S. Mantri, J. Daniels, Domain walls in ferroelectrics, J. Am. Ceram. Soc. 104 (2021) 1619–1632, https://doi.org/10.1111/jace.17555.

[21] F. Rubio-Marcos, A. Del Campo, R. López-Juárez, J.J. Romero, J.F. Fernández, High spatial resolution structure of $(K,Na)NbO_3$ lead-free ferroelectric domains, J. Mater. Chem. 22 (2012) 9714–9720, https://doi.org/10.1039/c2jm30483j.

[22] M. Bah, N. Alyabyeva, R. Retoux, F. Giovannelli, M. Zaghrioui, A. Ruyter, F. Delorme, I. Monot-Laffez, Investigation of the domain structure and hierarchy in potassium-sodium niobate lead-free piezoelectric single crystals, RSC Adv. 6 (2016) 49060–49067, https://doi.org/10.1039/c6ra07205d.

[23] Y. Qin, J. Zhang, W. Yao, C. Wang, S. Zhang, Domain structure of potassium-sodium niobate ceramics before and after poling, J. Am. Ceram. Soc. 98 (2015) 1027–1033, https://doi.org/10.1111/jace.13373.

[24] Y. Qin, J. Zhang, Y. Gao, Y. Tan, C. Wang, Study of domain structure of poled (K, Na)NbO_3 ceramics, J. Appl. Phys. 113 (2013) 204107, https://doi.org/10.1063/1.4807919.

[25] Y.X. Liu, W. Qu, H.C. Thong, Y. Zhang, Y. Zhang, F.Z. Yao, T.N. Nguyen, J.W. Li, M. H. Zhang, J.F. Li, B. Han, W. Gong, H. Wu, C. Wu, B. Xu, K. Wang, Isolated-oxygen-vacancy hardening in lead-free piezoelectrics, Adv. Mater. 34 (2022) 2202558, https://doi.org/10.1002/adma.202202558.

[26] J. Hirohashi, K. Yamada, H. Kamio, M. Uchida, S. Shichijyo, Control of specific domain structure in $KNbO_3$ single crystals by differential vector poling method, J. Appl. Phys. 98 (2005) 034107, https://doi.org/10.1063/1.2001148.

[27] W.T. Lee, E.K.H. Salje, U. Bismayer, Surface structure of domain walls in a ferroelastic system with a domain wall pressure, J. Phys. Condens. Matter 14 (2002) 7901–7910, https://doi.org/10.1088/0953-8984/14/34/308.

[28] D. Torres-Torres, A. Hurtado-Macias, R. Herrera-Basurto, E. Conteras, S. Sánchez, F. Mercader-Trejo, J. González-Hernández, O. Auciello, Anisotropic behavior of mechanical properties for the a- and c-domains in a (001) $BaTiO_3$ single crystal, J. Phys. Condens. Matter 35 (2023) 355703, https://doi.org/10.1088/1361-648X/acda08.

[29] Z. Tan, Y. Peng, J. An, Q. Zhang, J. Zhu, Intrinsic origin of enhanced piezoelectricity in alkali niobate-based lead-free ceramics, J. Am. Ceram. Soc. 102 (2019) 5262–5270, https://doi.org/10.1111/jace.16365.